Available online at www.sciencedirect.com
SCIENCE DIRECT®
International Journal of Heat and Fluid Flow 24 (2003) 874–887
International Journal of HEAT AND FLUID FLOW
www.elsevier.com/locate/ijhff

Combined forced and free flow in a vertical rectangular duct with prescribed wall heat flux

A. Barletta *, E. Rossi di Schio, E. Zanchini

Dipartimento di Ingegneria Energetica, Nucleare e del Controllo Ambientale (DIENCA), Università di Bologna, Viale Risorgimento 2, I-40136 Bologna, Italy

Received 9 July 2002; accepted 28 May 2003

Abstract

In this paper, combined forced and free convection is studied in a vertical rectangular duct with a prescribed uniform wall heat flux (H2 boundary condition). A different heat flux value for each plane wall is considered; the condition of a uniform wall heat flux throughout the duct results as a special case. The local momentum and energy balance equations are written in a dimensionless form and solved numerically, by means of a Galerkin finite element method. The numerical solution gives the dimensionless velocity and temperature distributions, together with the values of the Fanning friction factor, of the Nusselt number, of the momentum flux correction factor and of the kinetic energy correction factor. These dimensionless parameters are reported as functions of the aspect ratio and of the ratio between the Grashof number, Gr, and the Reynolds number, Re. The threshold values of Gr/Re for the onset of flow reversal are evaluated.

Keywords: Laminar flow; Mixed convection; Rectangular duct; Finite element methods

1. Introduction

The investigation of convection in non-circular ducts with a prescribed wall heating requires distinct boundary conditions, namely the H1 boundary condition and the H2 boundary condition. As is well known, the former corresponds to an axially uniform wall heat flux with a peripherally uniform wall temperature, while the latter corresponds to an axially and peripherally uniform wall heat flux. Sometimes, the concept of H2 boundary condition is extended, i.e. the wall heat flux is assumed to be axially uniform but peripherally piecewise uniform. Therefore, in the case of a rectangular duct, the H2 boundary conditions imply that the heat flux assumes either the same value on all the walls of the duct or a different value on each wall. Boundary conditions of kind H2 are good models for the thermal analysis of heating/cooling devices where no important axial change of the wall heat flux occurs, and the thermal conductivity of the wall is not very high. For instance, applications can be found in solar collector design and thermal control of electronic equipments.

In the literature, many authors have analysed the forced or mixed convection in rectangular ducts; most of the papers on this subject have been reviewed by Hartnett and Kostic (1989). In the last decade, some authors have studied the combined forced and free convection in rectangular ducts by employing numerical or experimental methods. In particular, the occurrence of flow reversal in a vertical heated channel has been studied experimentally through flow visualization (Gau et al., 1992). Cheng et al. (1995) have studied numerically the inlet region of a vertical rectangular duct with one wall kept at a higher temperature and the others at a lower temperature. Recently, the study has been extended to the case of two or more walls kept at a higher temperature (Cheng et al., 2000). Lee (1999) has utilized the velocity–vorticity formulation to solve numerically the balance equations in the case of natural convection in a vertical rectangular duct with three adiabatic walls and the last one isothermal or subjected to a uniform heat flux. In Hwang et al. (2001), the stream function method

* Corresponding author. Tel.: +39-51-2093281; fax: +39-51-2093296.
E-mail addresses: antonio.barletta@unibo.it (A. Barletta), eugenia.rossidischio@unibo.it (E. Rossi di Schio), enzo.zanchini@unibo.it (E. Zanchini).

0142-727X/$ - see front matter © 2003 Elsevier Inc. All rights reserved.
doi:10.1016/S0142-727X(03)00090-0

Nomenclature

a, b	lengths of the rectangle sides
c_1, c_2, c_3, c_4	real coefficients, defined by Eq. (4)
D	$2ab/(a+b)$, hydraulic diameter
f	Fanning friction factor, defined by Eq. (30)
g	magnitude of the gravitational acceleration
Gr	Grashof number, defined in Eq. (20)
$(Gr/Re)'$	threshold value of Gr/Re for the onset of flow reversal
h	average convection coefficient, defined in Eq. (32)
k	thermal conductivity
K_d	momentum flux correction factor, defined by Eq. (36)
K_e	kinetic energy correction factor, defined by Eq. (37)
Nu	Nusselt number, defined in Eq. (32)
Nu^*	modified Nusselt number, defined by Eq. (39)
p	pressure
P	difference between the pressure and the hydrostatic pressure
q_0	wall heat flux per unit area
$\bar{q}_w$	average wall heat flux per unit area
$\bar{q}^*_w$	modified average wall heat flux per unit area
Re	Reynolds number, defined in Eq. (20)
t	dimensionless temperature, defined in Eq. (20)
t_b	dimensionless bulk temperature, defined by Eq. (35)
$\bar{t}_w$	dimensionless average wall temperature, defined by Eq. (34)
T	temperature
T_b	bulk temperature in a duct section
T_0	mean temperature in a duct section, defined by Eq. (6)
$\overline{T}_w$	average wall temperature
$\overline{T}^*_w$	modified average wall temperature, defined by Eq. (38)
u	U/U_0, dimensionless velocity
U	Z-component of the fluid velocity
U_0	mean fluid velocity in a duct section, defined by Eq. (10)
x, y	dimensionless coordinates, defined in Eq. (20)
X, Y, Z	rectangular coordinates
Greeks	
α	thermal diffusivity
β	volumetric coefficient of thermal expansion
ΔT	$q_0 D/k$, reference temperature difference
λ	dimensionless parameter, defined in Eq. (20)
η	dimensionless parameter, defined in Eq. (20)
μ	dynamic viscosity
ν	kinematic viscosity
ϱ	mass density
ϱ_0	mass density for $T = T_0$
σ	b/a, aspect ratio
$\bar{\tau}_w$	average wall shear stress, defined by Eq. (29)

has been employed to solve numerically the governing equations for mixed convection in a horizontal square duct or in a horizontal circular tube. Moreover, some analytical solutions for laminar convection in vertical rectangular ducts are available in the recent literature. In particular, the free convection regime has been studied by Mc Bain (1999), for a duct with two isothermal and two adiabatic walls. On the other hand, forced convection has been studied by Spiga and Morini (1996) with reference to the eight H2 boundary conditions defined by Gao and Hartnett (1993). Two analytical solutions for mixed convection flow in a vertical rectangular duct have been recently presented by Barletta (2001, 2002). Barletta (2001) has considered a class of boundary conditions such that at least one wall of the duct is kept isothermal. On the other hand, Barletta (2002) has analysed the H1 boundary condition.

The aim of the present paper is to study the fully developed mixed convection in a vertical rectangular duct, with H2 boundary conditions. In the mathematical model, it will be assumed that the prescribed heat flux has a different value on each wall of the duct. In the examples, the case of a rectangular duct with an aspect ratio σ strictly less than 1 will be discussed by considering the same value of the heat flux on all the walls of the duct, while the case of a square duct ($\sigma = 1$) will be discussed for all the eight H2 boundary conditions defined by Gao and Hartnett (1993). The momentum and energy balance equations will be written in a dimensionless form and then solved numerically by means of a Galerkin finite element method. To implement the numerical code, the software package FlexPDE (© PDE-Solutions, Inc.) will be used. The solution will be compared with those available in the literature for the forced convection regime, in order to check the reliability and the precision of the numerical code.

2. Mathematical model

Let us consider a Newtonian fluid which flows steadily in a vertical duct with an infinite length and a rectangular cross-section. A drawing of the duct section and of the chosen coordinate axes (X, Y) is reported in Fig. 1. Let us assume that the flow is laminar and parallel, so that only the Z-component U of the velocity

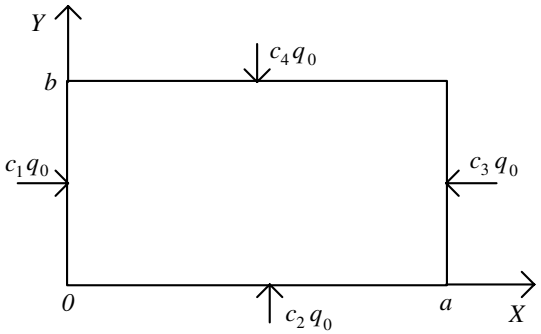

Fig. 1. Drawing of the duct section and of the thermal boundary conditions.

vector **U** is non-zero. The thermal conductivity k, the thermal diffusivity α and the dynamic viscosity μ of the fluid are treated as constants. The effect of viscous dissipation in the fluid is neglected, and the Boussinesq approximation is employed. Since this approximation implies that the velocity field is solenoidal, one has $\partial U/\partial Z = 0$, i.e. $U = U(X, Y)$. On account of the above assumptions, the momentum balance equation and the energy balance equation yield

$$\frac{\partial P}{\partial X} = 0, \quad \frac{\partial P}{\partial Y} = 0, \tag{1}$$

$$\varrho_0 g\beta(T - T_0) - \frac{\partial P}{\partial Z} + \mu\left(\frac{\partial^2 U}{\partial X^2} + \frac{\partial^2 U}{\partial Y^2}\right) = 0, \tag{2}$$

$$U\frac{\partial T}{\partial Z} = \alpha\left(\frac{\partial^2 T}{\partial X^2} + \frac{\partial^2 T}{\partial Y^2} + \frac{\partial^2 T}{\partial Z^2}\right), \tag{3}$$

where $P = p + \varrho_0 gZ$ is the difference between the pressure and the hydrostatic pressure. As a consequence of Eq. (1), P depends only on Z. The thermal boundary conditions, described also in Fig. 1, can be written in the form

$$\begin{aligned} &-k\frac{\partial T}{\partial X}\bigg|_{X=0} = c_1 q_0, \quad -k\frac{\partial T}{\partial Y}\bigg|_{Y=0} = c_2 q_0, \\ &k\frac{\partial T}{\partial X}\bigg|_{X=a} = c_3 q_0, \quad k\frac{\partial T}{\partial Y}\bigg|_{Y=b} = c_4 q_0, \end{aligned} \tag{4}$$

where c_1, c_2, c_3, c_4 are arbitrary real coefficients and q_0 is a prescribed wall heat flux per unit area. If $c_1 = c_2 = c_3 = c_4 = 1$, the duct is subjected to a uniform heat flux q_0 on all the walls. In this case, if q_0 is positive the duct is heated. By employing Eq. (4), one can obtain the eight H2 boundary conditions, usually denoted as **4**, **3L**, **3S**, **2L**, **2S**, **2C**, **1L** and **1S**, defined by Gao and Hartnett (1993). The values of the coefficients c_1, c_2, c_3, c_4 which correspond to these eight cases are reported in Table 1. The reference temperature T_0 must be chosen so that the linear equation of state

$$\varrho = \varrho_0[1 - \beta(T - T_0)] \tag{5}$$

Table 1
Values of c_1, c_2, c_3 and c_4 for the eight H2 thermal boundary conditions defined by Gao and Hartnett (1993)

	c_1	c_2	c_3	c_4
4	1	1	1	1
3L	1	1	0	1
3S	1	1	1	0
2L	0	1	0	1
2S	1	0	1	0
2C	1	1	0	0
1L	0	1	0	0
1S	1	0	0	0

is satisfied with the highest accuracy. Barletta and Zanchini (1999) have shown that the best choice of T_0 is the mean fluid temperature in a cross-section, namely

$$T_0 = \frac{1}{ab}\int_0^a \mathrm{d}X \int_0^b \mathrm{d}Y\, T(X, Y, Z). \tag{6}$$

By differentiating Eq. (2) with respect to Z, one obtains

$$\frac{\partial T}{\partial Z} = \frac{\mathrm{d}T_0}{\mathrm{d}Z} + \frac{1}{\varrho_0 g\beta}\frac{\mathrm{d}^2 P}{\mathrm{d}Z^2}. \tag{7}$$

Eq. (7) implies that $\partial T/\partial Z$ depends only on Z. By differentiating Eq. (6) with respect to Z, one obtains

$$\frac{\mathrm{d}T_0}{\mathrm{d}Z} = \frac{1}{ab}\int_0^a \mathrm{d}X \int_0^b \mathrm{d}Y \frac{\partial T}{\partial Z} = \frac{\partial T}{\partial Z}. \tag{8}$$

Eqs. (7) and (8) imply that $\mathrm{d}^2 P/\mathrm{d}Z^2 = 0$, i.e. that $\mathrm{d}P/\mathrm{d}Z$ is a constant. Eq. (3) can be rewritten as

$$U\frac{\mathrm{d}T_0}{\mathrm{d}Z} = \alpha\left(\frac{\partial^2 T}{\partial X^2} + \frac{\partial^2 T}{\partial Y^2} + \frac{\mathrm{d}^2 T_0}{\mathrm{d}Z^2}\right). \tag{9}$$

The mean velocity U_0 in a duct cross-section is defined by the relation

$$U_0 = \frac{1}{ab}\int_0^a \mathrm{d}X \int_0^b \mathrm{d}Y\, U(X, Y). \tag{10}$$

By integrating Eq. (9) with respect to X and Y in a duct cross-section, and by taking into account Eq. (10) and the boundary conditions (4), one obtains

$$U_0\frac{\mathrm{d}T_0}{\mathrm{d}Z} - \alpha\frac{\mathrm{d}^2 T_0}{\mathrm{d}Z^2} = \frac{\alpha q_0}{kab}[(c_1 + c_3)b + (c_2 + c_4)a]. \tag{11}$$

By introducing the hydraulic diameter $D = 2ab/(a + b)$ and the mean value of the wall heat flux $\bar{q}_\mathrm{w}$, defined by

$$\bar{q}_\mathrm{w} = q_0\frac{(c_1 + c_3)b + (c_2 + c_4)a}{2(a + b)}, \tag{12}$$

one can rewrite Eq. (11) as

$$U_0\frac{\mathrm{d}T_0}{\mathrm{d}Z} - \alpha\frac{\mathrm{d}^2 T_0}{\mathrm{d}Z^2} = \frac{4\alpha\bar{q}_\mathrm{w}}{kD}. \tag{13}$$

Since $\partial T/\partial Z$ is independent of X and Y, by differentiating Eq. (9) with respect to Z one obtains

$$U\frac{\mathrm{d}^2 T_0}{\mathrm{d}Z^2} = \alpha\frac{\mathrm{d}^3 T_0}{\mathrm{d}Z^3}. \tag{14}$$

Moreover, by differentiating Eq. (13) with respect to Z one is led to the equation

$$U_0 \frac{\mathrm{d}^2 T_0}{\mathrm{d}Z^2} = \alpha \frac{\mathrm{d}^3 T_0}{\mathrm{d}Z^3}. \tag{15}$$

A comparison between Eqs. (14) and (15) yields

$$(U - U_0) \frac{\mathrm{d}^2 T_0}{\mathrm{d}Z^2} = 0. \tag{16}$$

Since $U - U_0$ cannot vanish because $U_0 \neq 0$ and the velocity is zero at the duct walls, one reaches the conclusion

$$\frac{\mathrm{d}^2 T_0}{\mathrm{d}Z^2} = 0. \tag{17}$$

Eqs. (13) and (17) yield

$$\frac{\mathrm{d}T_0}{\mathrm{d}Z} = \frac{4\alpha \bar{q}_\mathrm{w}}{kDU_0}. \tag{18}$$

By substituting Eqs. (17) and (18) into Eq. (9), one obtains

$$\frac{\partial^2 T}{\partial X^2} + \frac{\partial^2 T}{\partial Y^2} = \frac{4\bar{q}_\mathrm{w}}{kDU_0} U. \tag{19}$$

Let us define the following dimensionless variables:

$$\begin{gathered} x = \frac{X}{a}, \quad y = \frac{Y}{a}, \quad \sigma = \frac{b}{a}, \quad u = \frac{U}{U_0}, \\ \eta = \frac{\bar{q}_\mathrm{w}}{q_0} = \frac{(c_1 + c_3)\sigma + c_2 + c_4}{2(1+\sigma)}, \quad t = \frac{T - T_0}{\Delta T}, \\ Re = \frac{U_0 D}{\nu}, \quad Gr = \frac{g\beta \Delta T D^3}{\nu^2}, \quad \lambda = -\frac{a^2}{\mu U_0} \frac{\mathrm{d}P}{\mathrm{d}Z}, \end{gathered} \tag{20}$$

where the reference temperature difference ΔT is given by

$$\Delta T = \frac{q_0 D}{k}. \tag{21}$$

It will be assumed, without loss of generality, that the parameter η is always positive, so that $\bar{q}_\mathrm{w}$ and q_0 have the same sign.

The ratio between the Reynolds number and the Grashof number is

$$\frac{Gr}{Re} = \frac{g\beta \Delta T D^2}{\nu U_0}. \tag{22}$$

Since $\partial T/\partial Z = \mathrm{d}T_0/\mathrm{d}Z$, then $t = t(x,y)$. On account of Eqs. (20) and (21), Eqs. (2) and (19) can be written in the dimensionless form

$$\frac{\partial^2 u}{\partial x^2} + \frac{\partial^2 u}{\partial y^2} + \frac{Gr}{Re} \frac{(1+\sigma)^2}{4\sigma^2} t + \lambda = 0, \tag{23}$$

$$\frac{\partial^2 t}{\partial x^2} + \frac{\partial^2 t}{\partial y^2} = \frac{(1+\sigma)^2}{\sigma^2} \eta u. \tag{24}$$

The boundary conditions for the dimensionless velocity distribution u are as follows:

$$u(0,y) = u(1,y) = u(x,0) = u(x,\sigma) = 0. \tag{25}$$

By employing Eqs. (20) and (21), one can write the thermal boundary conditions (4) in the dimensionless form

$$\begin{aligned} &\left.\frac{\partial t}{\partial x}\right|_{x=0} = -\frac{1+\sigma}{2\sigma} c_1, \quad \left.\frac{\partial t}{\partial y}\right|_{y=0} = -\frac{1+\sigma}{2\sigma} c_2, \\ &\left.\frac{\partial t}{\partial x}\right|_{x=1} = \frac{1+\sigma}{2\sigma} c_3, \quad \left.\frac{\partial t}{\partial y}\right|_{y=\sigma} = \frac{1+\sigma}{2\sigma} c_4. \end{aligned} \tag{26}$$

On account of Eq. (10), one can obtain the following constraint for the velocity distribution u:

$$\int_0^1 \mathrm{d}x \int_0^\sigma \mathrm{d}y\, u(x,y) = \sigma. \tag{27}$$

Moreover, Eq. (6) yields the following constraint for the temperature distribution t:

$$\int_0^1 \mathrm{d}x \int_0^\sigma \mathrm{d}y\, t(x,y) = 0. \tag{28}$$

Eqs. (23)–(28) show that the dimensionless fields $u(x,y)$ and $t(x,y)$, as well as the dimensionless parameter λ, depend only on the prescribed values of σ, c_1, c_2, c_3, c_4 and Gr/Re. As a consequence, for fixed values of σ, c_1, c_2, c_3, c_4 and Gr/Re, the fields $u(x,y)$, $t(x,y)$ and the parameter λ obtained for heated duct ($q_0 > 0$) and upward flow ($U_0 > 0$) coincide with those obtained for cooled duct ($q_0 < 0$) and downward flow ($U_0 < 0$). Moreover, the fields $u(x,y)$, $t(x,y)$ and the parameter λ obtained for heated duct ($q_0 > 0$) and downward flow ($U_0 < 0$) coincide with those obtained for cooled duct ($q_0 < 0$) and upward flow ($U_0 > 0$). As it will be shown in Sections 3 and 4, for negative values of the ratio Gr/Re, the flow-reversal phenomenon may occur. As is well known, this phenomenon corresponds to negative local values of u, i.e. to a local velocity with a direction opposite to that of the mean flow. For instance, negative values of Gr/Re can correspond to $q_0 < 0$ and $U_0 > 0$. In this case, if one considers the boundary condition **4** and if $|Gr/Re|$ exceeds a threshold value, the fluid density next to the boundary becomes much higher than the mean fluid density and local downward flow may occur in the neighbourhood of the boundary.

The average wall shear stress is given by

$$\begin{aligned} \bar{\tau}_\mathrm{w} = \frac{\mu}{2(a+b)} \Bigg[&\int_0^b \mathrm{d}Y \left.\frac{\partial U}{\partial X}\right|_{X=0} - \int_0^b \mathrm{d}Y \left.\frac{\partial U}{\partial X}\right|_{X=a} \\ &+ \int_0^a \mathrm{d}X \left.\frac{\partial U}{\partial Y}\right|_{Y=0} - \int_0^a \mathrm{d}X \left.\frac{\partial U}{\partial Y}\right|_{Y=b} \Bigg]. \end{aligned} \tag{29}$$

On account of Eqs. (20) and (29), one can define the Fanning friction factor as

$$f=\frac{2\bar{\tau}_{\mathrm{w}}}{\varrho_0 U_0^2}$$
$$=\frac{2\sigma}{(1+\sigma)^2 Re}\left[\int_0^\sigma \mathrm{d}y\left.\frac{\partial u}{\partial x}\right|_{x=0}-\int_0^\sigma \mathrm{d}y\left.\frac{\partial u}{\partial x}\right|_{x=1}+\int_0^1 \mathrm{d}x\left.\frac{\partial u}{\partial y}\right|_{y=0}-\int_0^1 \mathrm{d}x\left.\frac{\partial u}{\partial y}\right|_{y=\sigma}\right]. \quad (30)$$

It can be easily shown that, as a consequence of Eqs. (23), (28) and (30), the parameters f and λ are related through the expression

$$f\,Re=\frac{2\sigma^2\lambda}{(1+\sigma)^2}. \quad (31)$$

The mean Nusselt number in a duct cross-section can be defined by the relation

$$Nu=\frac{hD}{k}=\frac{\bar{q}_{\mathrm{w}}D}{k(\overline{T}_{\mathrm{w}}-T_b)}, \quad (32)$$

where h is the average convection coefficient, $\bar{q}_{\mathrm{w}}$ is the average wall heat flux, defined by Eq. (12), $\overline{T}_{\mathrm{w}}$ is the average wall temperature in a duct section and T_{b} is the bulk temperature. By introducing the dimensionless quantities defined by Eqs. (20) and (21) into Eq. (32), one obtains

$$Nu=\frac{\eta}{\bar{t}_{\mathrm{w}}-t_{\mathrm{b}}}, \quad (33)$$

where $\bar{t}_{\mathrm{w}}$ is the mean value of the dimensionless wall temperature, namely

$$\bar{t}_{\mathrm{w}}=\frac{1}{2(1+\sigma)}\left[\int_0^1 \mathrm{d}x\,t(x,0)+\int_0^\sigma \mathrm{d}y\,t(1,y)+\int_0^1 \mathrm{d}x\,t(x,\sigma)+\int_0^\sigma \mathrm{d}y\,t(0,y)\right] \quad (34)$$

and t_{b} is the dimensionless bulk temperature, namely

$$t_{\mathrm{b}}=\frac{1}{\sigma}\int_0^1 \mathrm{d}x\int_0^\sigma \mathrm{d}y\,tu. \quad (35)$$

Finally, the momentum flux correction factor and the kinetic energy correction factor (Shah and London, 1978) are given by

$$K_{\mathrm{d}}=\frac{1}{ab}\int_0^a \mathrm{d}X\int_0^b \mathrm{d}Y\left(\frac{U}{U_0}\right)^2=\frac{1}{\sigma}\int_0^1 \mathrm{d}x\int_0^\sigma \mathrm{d}y\,u^2, \quad (36)$$

$$K_{\mathrm{e}}=\frac{1}{ab}\int_0^a \mathrm{d}X\int_0^b \mathrm{d}Y\left(\frac{U}{U_0}\right)^3=\frac{1}{\sigma}\int_0^1 \mathrm{d}x\int_0^\sigma \mathrm{d}y\,u^3. \quad (37)$$

3. Boundary condition H2 of kind 4: Fanning friction factor and Nusselt number

The momentum and energy balance equations (23) and (24), together with the boundary conditions (25), (26) and the constraints (27), (28), have been solved numerically for given values of the parameters σ, c_1, c_2, c_3, c_4 and Gr/Re. The software package FlexPDE Version 3.01 (© PDESolutions Inc.) has been employed in order to build the computational grid, to map Eqs. (23)–(28) into a linear system of algebraic equations and to solve this system. This software solves partial differential equations by utilizing a Galerkin finite element method. The spatial domain under assumption, i.e. the rectangle $[0,1]\times[0,\sigma]$, is divided into triangular elements and the grid is iteratively refined until a prescribed value of the accuracy parameter "`errlim`" defined by the software is reached. The numerical solutions have been checked in order to obtain values of Nu, $f\,Re$, K_{d} and K_{e} independent of the grid as well as of the value of the accuracy parameter.

In this section, the boundary condition H2 of kind **4** is considered ($c_1=c_2=c_3=c_4=1$). Three different examples, given by three different values of the aspect ratio σ, are discussed: $\sigma=1$, $\sigma=0.5$ and $\sigma=0.2$.

Table 2 refers to $Gr/Re=0$, i.e. to forced convection, and reports a comparison between the values of the

Table 2
Comparison between the values of $f\,Re$ and of Nu available in the literature and those obtained in the present paper, for $Gr/Re=0$

σ	Present paper		Shah and London (1978)		Spiga and Morini (1996)
	$f\,Re$	Nu	$f\,Re$	Nu	Nu
1/10	21.1689	2.9061	21.16888	2.95	2.907
1/9	20.9039	2.9065	20.90385	2.94	–
1/8	20.5847	2.9074	20.58464	2.94	2.909
1/7	20.1931	2.9092	20.19310	2.94	–
1/6	19.7022	2.9126	19.70220	2.93	–
1/5	19.0705	2.9192	19.07050	2.93	2.922
1/4	18.2328	2.9326	18.23278	2.94	2.935
1/3	17.0897	2.9608	17.08967	2.97	2.964
1/2	15.5481	3.0192	15.54806	3.02	3.022
1	14.2271	3.0874	14.22708	3.091	3.091

Fanning friction factor and of the Nusselt number obtained in the present paper and those reported by Shah and London (1978) and by Spiga and Morini (1996). The values presented in Table 2 refer to several aspect ratios. The comparison reveals a very good agreement between the values of the friction factor obtained in the present paper and those presented by Shah and London (1978), while the values of the Nusselt number obtained in the present paper slightly differ from those reported by Shah and London (1978). However, the agreement with the values of the Nusselt number obtained analytically by Spiga and Morini (1996) is very good, since the first three digits are coincident. Indeed, the results reported by Shah and London (1978) for the Fanning friction factor were obtained by solving the balance equations analytically, while those for the Nusselt number were obtained numerically.

Table 3
Values of $f\,Re$, Nu, K_d and K_e for a square duct ($\sigma = 1$), for the boundary condition H2 of kind **4**

Gr/Re	$f\,Re$	Nu	K_d	K_e
−200	3.617	2.545	1.789	3.785
−100	9.085	2.743	1.547	2.795
0	14.23	3.087	1.378	2.154
100	18.67	3.423	1.273	1.778
200	22.82	3.630	1.204	1.550
300	25.70	4.156	1.171	1.449
400	31.34	3.794	1.138	1.361
500	36.26	3.763	1.139	1.378
600	31.19	5.763	1.138	1.359

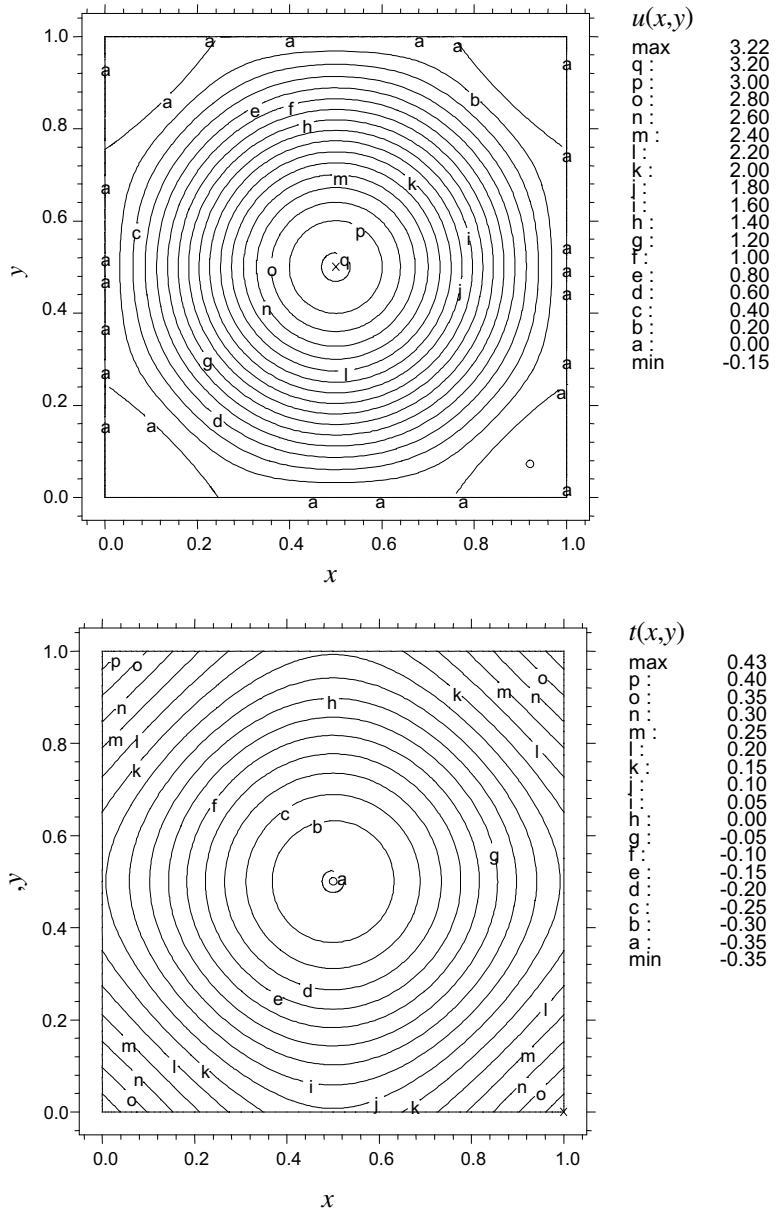

Fig. 2. Contour plots of $u(x,y)$ (upper frame) and $t(x,y)$ (lower frame) for $\sigma = 1$ and $Gr/Re = -250$; boundary condition H2 of kind **4**.

Table 3 refers to the case $\sigma = 1$ and reports the values of the Fanning friction factor, of the Nusselt number and of the correction factors K_d and K_e, for Gr/Re in the range $-200 \leqslant Gr/Re \leqslant 600$. This table shows that $f\,Re$, Nu, K_d and K_e are non-monotonic functions of the parameter Gr/Re. In particular, $f\,Re$ first increases and then decreases, reaching a local maximum for $Gr/Re \approx 500$. The Nusselt number presents a local maximum for $Gr/Re \approx 300$ and a local minimum for $Gr/Re \approx 500$. Both K_d and K_e display a local minimum for $Gr/Re \approx 400$ and a local maximum for $Gr/Re \approx 500$.

In the case $\sigma = 1$, the threshold value for the onset of flow reversal is $(Gr/Re)' \approx -100$. This value is almost coincident with the threshold value for the onset of flow reversal which has been found for the H1 boundary condition (Barletta, 2002).

Fig. 2 represents the contour lines of the dimensionless velocity and temperature distributions, for $\sigma = 1$ and $Gr/Re = -250$. On the other hand, Fig. 3 refers to $\sigma = 1$ and $Gr/Re = 600$. The upper frame of Fig. 2 refers to the dimensionless velocity distribution and reveals that, in correspondence to the four corners of the duct section, regions of flow reversal exist. The upper frame of Fig. 3 shows that the velocity distribution strongly differs from the case of forced convection. In particular, the figure reveals the existence of four local maxima and

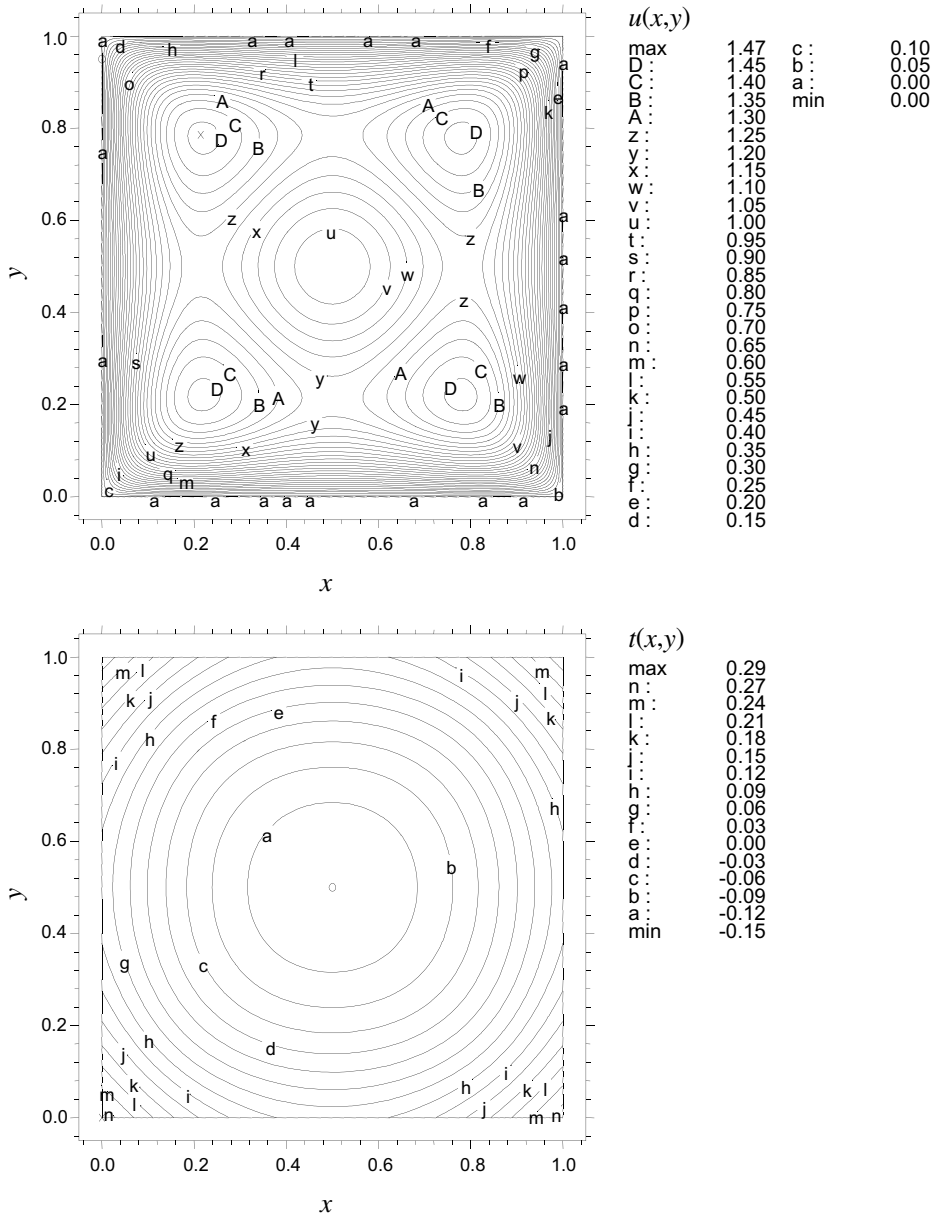

Fig. 3. Contour plots of $u(x,y)$ (upper frame) and $t(x,y)$ (lower frame) for $\sigma = 1$ and $Gr/Re = 600$; boundary condition H2 of kind **4**.

of a local minimum at the centre of the duct. The lower frames of Figs. 2 and 3 point out that the wall temperature is not uniform, and that the dimensionless temperature assumes its minimum value at the centre of the duct and its maximum value at the boundary corners. The latter circumstance is the reason why the flow reversal regions for $Gr/Re = -250$ take place in correspondence of the four boundary corners. Since the wall temperature is definitely not uniform, the H2 boundary condition (peripherally uniform wall heat flux) is quite distinct from the H1 boundary condition (peripherally uniform wall temperature).

Figs. 4 and 5 display the contour lines of the dimensionless velocity and temperature distributions, for $\sigma = 0.5$ and $Gr/Re = -180$ (Fig. 4) or $Gr/Re = 500$ (Fig. 5). In the upper frame of Fig. 4, two large regions of flow reversal are evident, close to the shorter walls of the boundary. An analysis of the lower frame of this figure leads to the conclusion that the heat flux in the X-direction is greater than the heat flux in the Y-direction, except close to the plane $x = 0.5$. In the upper frame of Fig. 5, two local maxima of the dimensionless velocity occur.

Table 4 displays values of $f\,Re$, Nu, K_d and K_e which refer to $\sigma = 0.5$, both for negative and for positive values of the ratio Gr/Re. The table shows that the parameters $f\,Re$ and Nu are increasing functions of Gr/Re, while K_d and K_e are decreasing functions. In the case

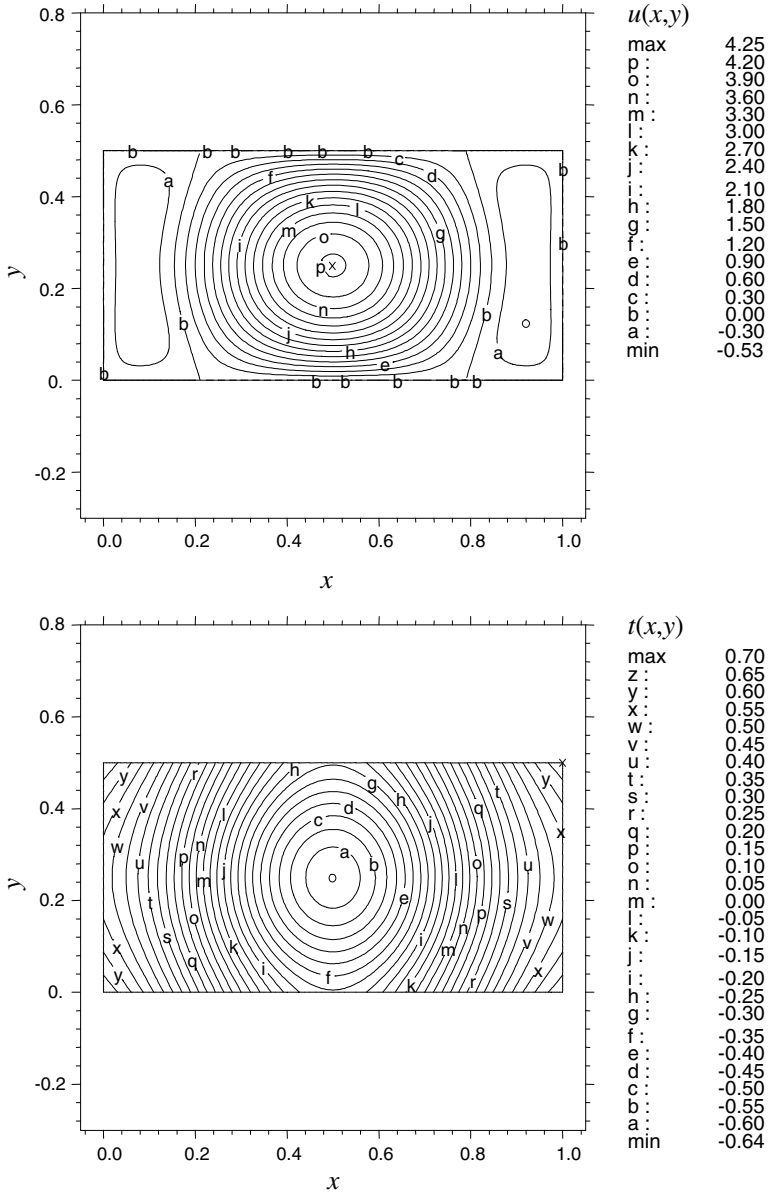

Fig. 4. Contour plots of $u(x, y)$ (upper frame) and $t(x, y)$ (lower frame) for $\sigma = 0.5$ and $Gr/Re = -180$; boundary condition H2 of kind **4**.

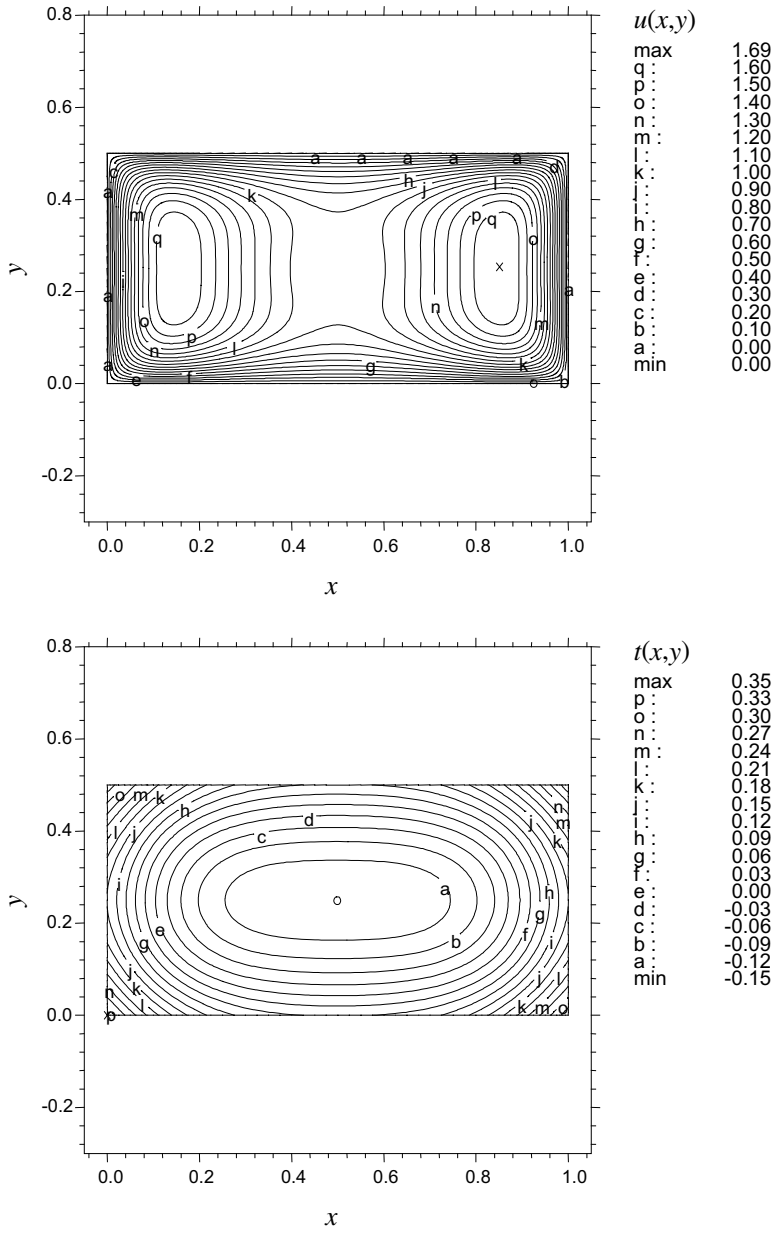

Fig. 5. Contour plots of $u(x,y)$ (upper frame) and $t(x,y)$ (lower frame) for $\sigma = 0.5$ and $Gr/Re = 500$; boundary condition H2 of kind **4**.

Table 4
Values of $f\,Re$, Nu, K_d and K_e for a rectangular duct with $\sigma = 0.5$, for the boundary condition H2 of kind **4**

Gr/Re	$f\,Re$	Nu	K_d	K_e
−180	1.348	1.300	2.924	8.802
−100	9.315	2.133	1.721	3.498
0	15.55	3.019	1.347	2.039
100	19.90	3.640	1.246	1.686
200	23.41	4.085	1.211	1.583
300	26.21	4.518	1.198	1.551
400	28.56	4.911	1.192	1.539
500	30.43	5.328	1.187	1.530
600	31.84	5.795	1.182	1.518

$\sigma = 0.5$, the onset of flow reversal occurs for $Gr/Re \approx -85$. This value is greater than the threshold value which has been determined for the H1 thermal boundary condition (Barletta, 2002). Moreover, for $\sigma = 0.2$ the threshold value for the onset of flow reversal is $(Gr/Re)' \approx -30$, and this value is much greater than that for the H1 thermal boundary condition (Barletta, 2002). One can point out that, while in the case of H1 thermal boundary condition $(Gr/Re)'$ is a monotonic increasing function of the aspect ratio σ, in the case of the H2 boundary condition $(Gr/Re)'$ is a decreasing function of σ.

Table 5
Values of $f\,Re$, Nu, K_d and K_e for a rectangular duct with $\sigma = 0.2$, for the boundary condition H2 of kind **4**

Gr/Re	$f\,Re$	Nu	K_d	K_e
−50	2.590	0.06508	20.18	99.55
−20	17.66	1.864	1.400	2.242
0	19.07	2.919	1.271	1.770
50	21.04	4.197	1.239	1.675
100	22.46	4.746	1.239	1.685
150	23.66	5.072	1.238	1.692
200	24.77	5.300	1.236	1.693

Finally, Table 5 displays values of $f\,Re$, Nu, K_d and K_e which refer to $\sigma = 0.2$, both for negative and for positive values of the ratio Gr/Re. As in the case $\sigma = 0.5$, the parameters $f\,Re$ and Nu are increasing functions of Gr/Re, while K_d is a decreasing function.

4. Other H2 boundary conditions for the square duct

In this section, the eight H2 thermal boundary conditions defined in Table 1 are investigated in the special case of a square duct, i.e. $\sigma = 1$. Obviously, for a square duct, the boundary condition **3L** coincides with **3S**, the boundary condition **2L** coincides with **2S**, while the boundary condition **1L** coincides with **1S**. The Fanning friction factor, the Nusselt number, as well as the momentum flux correction factor and the kinetic energy correction factor are evaluated for several values of Gr/Re. A comparison of the results obtained in the present paper with those available in the literature is performed. In particular, the paper by Spiga and Morini (1996), which refers to the special case of forced convection, is considered. In this paper, as well as in Gao and Hartnett (1993), different definitions of the average wall temperature and of the average wall heat flux have been provided, by taking into account only the contribution of the non-adiabatic walls of the duct. As a consequence, for the boundary conditions H2 defined in Table 1, the average wall temperature and the Nusselt number considered in Spiga and Morini (1996), as well as in Gao and Hartnett (1993), are given by

$$\overline{T}^*_w = \frac{1}{2(a+b)}\left[c_2\int_0^a \mathrm{d}X\,T(X,0) + c_3\int_0^b \mathrm{d}Y\,T(a,Y) + c_4\int_0^a \mathrm{d}X\,T(X,b) + c_1\int_0^b \mathrm{d}Y\,T(0,Y)\right], \quad (38)$$

$$Nu^* = \frac{\bar{q}^*_w D}{k(\overline{T}^*_w - T_b)}, \quad (39)$$

where $\bar{q}^*_w$ is the average wall heat flux of the non-adiabatic walls.

In Table 6, the values of the modified Nusselt number obtained in the present paper are compared with those obtained analytically and presented by Spiga and Morini (1996). As it can be easily checked, the values are in fair agreement, since the first three digits are coincident.

Table 6
Values of the modified Nusselt number for a square duct ($\sigma = 1$), in the case of forced convection

Boundary conditions	Nu^*, present paper	Nu^*, Spiga and Morini (1996)
4	3.0874	3.091
3L–3S	2.9399	2.943
2L–2S	4.0769	4.083
2C	2.4275	2.430
1L–1S	2.6835	2.686

In Tables 7 and 8, the values of $f\,Re$, Nu, K_d and K_e are reported, both for negative and for positive values of the ratio Gr/Re. The tables refer to the boundary condition **3L–3S** and to the boundary condition **2L–2S** respectively. These tables show that the parameters $f\,Re$ and Nu are increasing functions of Gr/Re, while K_d and K_e are decreasing functions of the same parameter. In the case **3L–3S**, the threshold value for the onset of flow reversal is $(Gr/Re)' \approx -75$, while in the case **2L–2S** one has $(Gr/Re)' \approx -180$.

Tables 9 and 10 provide the values of $f\,Re$, Nu, K_d and K_e both for negative and for positive values of the ratio Gr/Re. The tables refer to the boundary condition **2C** and to the boundary condition **1L–1S** respectively. In both cases, the parameters $f\,Re$ and Nu are increasing functions of Gr/Re, while K_d and K_e first decrease and

Table 7
Values of $f\,Re$, Nu, K_d and K_e for a square duct ($\sigma = 1$), for the boundary condition H2 of kind **3L–3S**

Gr/Re	$f\,Re$	Nu	K_d	K_e
−100	10.44	2.222	1.632	3.107
−50	12.39	2.746	1.451	2.423
0	14.23	3.087	1.378	2.154
100	17.62	3.534	1.316	1.931
200	20.66	3.870	1.287	1.834
300	23.53	4.127	1.271	1.788
400	25.70	4.498	1.258	1.750

Table 8
Values of $f\,Re$, Nu, K_d and K_e for a square duct ($\sigma = 1$), for the boundary condition H2 of kind **2L–2S**

Gr/Re	$f\,Re$	Nu	K_d	K_e
−150	10.44	2.789	1.501	2.613
−100	11.75	2.887	1.455	2.437
−50	13.01	2.988	1.414	2.285
0	14.23	3.087	1.378	2.154
100	16.53	3.285	1.321	1.946
200	18.67	3.485	1.277	1.793
300	20.66	3.688	1.245	1.685
400	22.50	3.898	1.223	1.613
500	24.19	4.119	1.208	1.566
600	25.70	4.353	1.199	1.539

Table 9
Values of $f\,Re$, Nu, K_d and K_e for a square duct ($\sigma = 1$), for the boundary condition H2 of kind **2C**

Gr/Re	$f\,Re$	Nu	K_d	K_e
−150	10.44	1.270	2.103	4.851
−100	11.75	1.887	1.626	3.070
−50	13.01	2.509	1.444	2.394
0	14.23	3.087	1.378	2.154
100	16.53	4.033	1.372	2.133
200	18.67	4.711	1.413	2.285
300	20.69	5.197	1.462	2.467
400	22.50	5.568	1.500	2.607
500	24.43	5.862	1.554	2.811
600	26.21	6.115	1.599	2.981

Table 10
Values of $f\,Re$, Nu, K_d and K_e for a square duct ($\sigma = 1$), for the boundary condition H2 of kind **1L–1S**

Gr/Re	$f\,Re$	Nu	K_d	K_e
−150	12.39	1.745	1.594	2.941
−100	13.01	2.148	1.474	2.503
−50	13.63	2.597	1.408	2.264
0	14.23	3.087	1.378	2.154
100	15.40	4.178	1.381	2.165
200	16.53	5.376	1.426	2.336
300	17.63	6.621	1.491	2.580
400	18.67	7.859	1.559	2.843
500	19.69	9.030	1.627	3.112
600	20.69	10.21	1.698	3.394

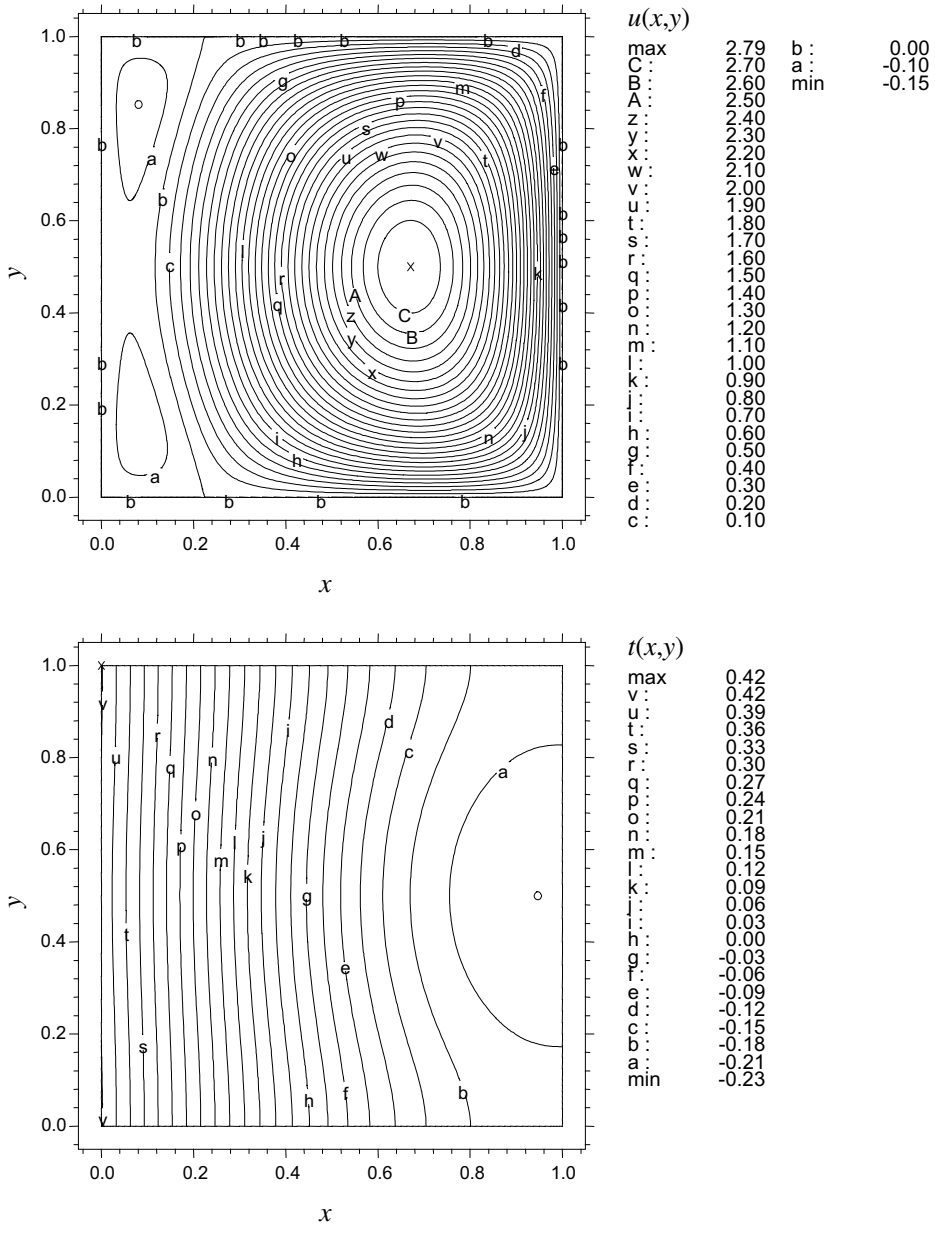

Fig. 6. Contour plots of $u(x,y)$ (upper frame) and $t(x,y)$ (lower frame) for $\sigma = 1$ and $Gr/Re = -200$; boundary condition H2 of kind **1L–1S**.

then increase. The minimum of K_d is reached for $Gr/Re \approx 100$ in both cases, while the minimum of K_e is reached for $Gr/Re \approx 100$ in case **2C** and for $Gr/Re \approx 0$ in case **1L**–**1S**. In case **2C**, the threshold value for the onset of flow reversal is $(Gr/Re)' \approx -50$, while in case **1L**–**1S** one has $(Gr/Re)' \approx -100$.

In Figs. 6–8, the contour lines of the dimensionless velocity and of the dimensionless temperature are reported for $Gr/Re = -200$ and for three different thermal boundary conditions, i.e. **1L**–**1S** (Fig. 6), **2C** (Fig. 7), and **2L**–**2S** (Fig. 8). In the upper frame of Figs. 6 and 7, regions of flow reversal are evident close to the non-adiabatic walls. The lower frames of Figs. 6–8 show that the dimensionless wall temperature is far from being uniform. In Figs. 6 and 7, the dimensionless temperature reaches its maximum in correspondence of the non-adiabatic walls. In the lower frame of Fig. 8, the maximum of the dimensionless temperature occurs at the centre of the duct section and the heat flux along the X-direction is almost everywhere greater than the heat flux along the Y-direction.

5. Convergence and grid independence of the numerical solution

For every H2 boundary condition examined, for all the values of Gr/Re and of σ which have been con-

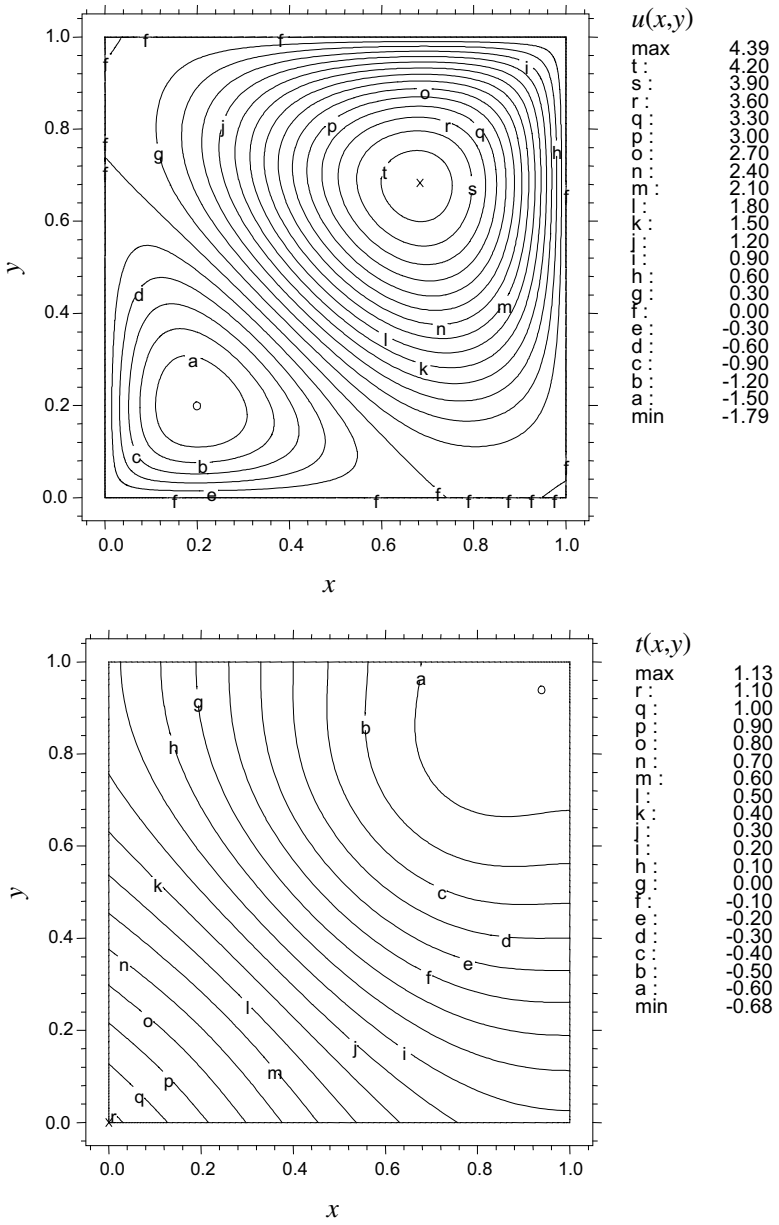

Fig. 7. Contour plots of $u(x, y)$ (upper frame) and $t(x, y)$ (lower frame) for $\sigma = 1$ and $Gr/Re = -200$; boundary condition H2 of kind **2C**.

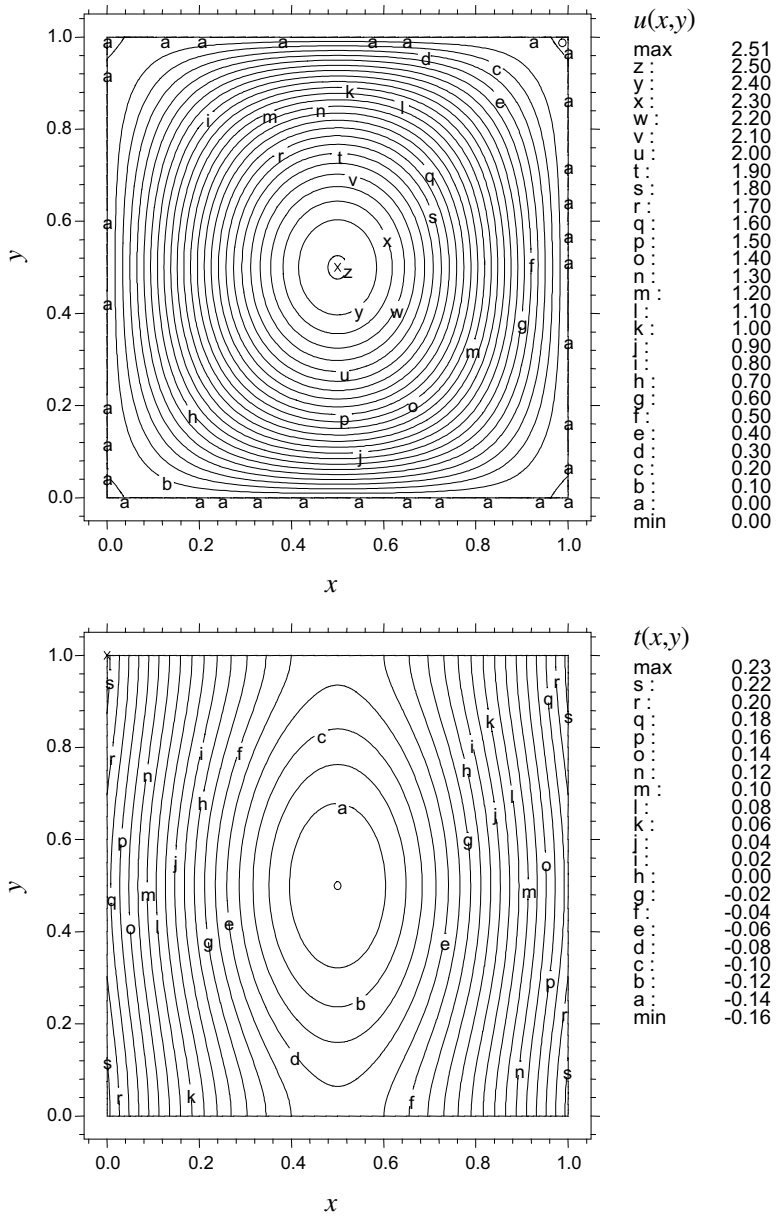

Fig. 8. Contour plots of $u(x,y)$ (upper frame) and $t(x,y)$ (lower frame) for $\sigma = 1$ and $Gr/Re = -200$; boundary condition H2 of kind **2L–2S**.

sidered, the convergence and the grid independence of the numerical solution have been checked, with reference to the parameters $f\,Re$, Nu, K_d and K_e. An example of these checks, for a square duct with $Gr/Re = -100$, is illustrated in Table 11. Indeed, this value of Gr/Re is rather critical from a numerical viewpoint, because it yields flow-reversal regions for almost all the boundary conditions which have been studied. In Table 11, three different gridding procedures have been considered: "grid", "grid×" and "grid+". The procedure "grid" builds an unstructured and unconstrained grid; the procedure "grid×" builds an unstructured grid which is constrained to have nodes which lie on the diagonals of the square; the procedure "grid+" builds an unstructured grid which is constrained to have nodes which lie on the apothems of the square. In Table 11, two different values of the accuracy parameter "`errlim`" are considered: 7×10^{-8} (higher accuracy) and 7×10^{-7} (lower accuracy). The table shows that, if the "`errlim`" parameter is sufficiently small, neither this parameter nor the gridding procedure has an important influence on the values of $f\,Re$ and Nu. In particular, if `errlim` $= 7\times10^{-8}$, the three gridding procedures yield values which agree within the first three digits and display a small oscillation of the fourth digit.

Table 11
Values of $f\,Re$ (plain text) and of Nu (in italic) for a square duct with $\sigma = 1$ and $Gr/Re = -100$, and for different boundary conditions; comparison between values obtained by means of different grids and different accuracies

Boundary conditions		errlim $= 7\times10^{-8}$			errlim $= 7\times10^{-7}$		
		grid	grid×	grid+	grid	grid×	grid+
4	$f\,Re$	9.089	9.082	9.085	9.114	9.085	9.124
	Nu	*2.743*	*2.737*	*2.745*	*2.768*	*2.745*	*2.763*
3L–3S	$f\,Re$	10.43	10.44	10.44	10.44	10.44	10.45
	Nu	*2.222*	*2.222*	*2.223*	*2.221*	*2.221*	*2.232*
2L–2S	$f\,Re$	11.75	11.75	11.75	11.75	11.77	11.77
	Nu	*2.887*	*2.888*	*2.887*	*2.891*	*2.914*	*2.915*
2C	$f\,Re$	11.75	11.75	11.75	11.75	11.75	11.77
	Nu	*1.887*	*1.886*	*1.887*	*1.886*	*1.887*	*1.915*
1L–1S	$f\,Re$	13.01	13.01	13.01	13.01	13.01	13.01
	Nu	*2.148*	*2.149*	*2.148*	*2.149*	*2.148*	*2.149*

6. Conclusions

An analysis of the fully developed mixed convection in a vertical rectangular duct has been performed. Reference has been made to the eight H2 thermal boundary conditions defined by Gao and Hartnett (1993), given by combinations of isoflux and adiabatic walls. The Boussinesq approximation has been employed and the mean temperature T_0 in a duct cross-section has been chosen as the reference temperature for the linearization of the equation of state $\varrho = \varrho(T)$. The momentum and energy balance equations have been written in a dimensionless form. It has been shown that both the dimensionless velocity $u(x, y)$ and the dimensionless temperature $t(x, y)$ are two-dimensional fields which depend only on the ratio Gr/Re, on the aspect ratio σ and on c_1, c_2, c_3, c_4. The set of dimensionless equations has been solved numerically, by means of a Galerkin finite element method implemented by utilizing the software package FlexPDE.

In the special case of forced convection, the results have been compared with those obtained by Spiga and Morini (1996) and by Shah and London (1978). The comparison has revealed a fair agreement between our results and those obtained analytically for the friction factor (Shah and London, 1978) and for the Nusselt number (Spiga and Morini, 1996).

The effect of buoyancy has been studied, and the values of the parameters $f\,Re$, Nu, K_d and K_e have been reported as functions of Gr/Re for different values of the aspect ratio σ. First, reference has been made to the H2 thermal boundary condition of kind **4**. Then, for the special case of a square duct, the other H2 boundary conditions have been investigated. It has been shown that, in each case, there exists a negative real number $(Gr/Re)'$ such that for $Gr/Re < (Gr/Re)'$ the phenomenon of flow reversal occurs. This is a well known effect which arises for mixed convection in vertical or inclined ducts, and implies the existence of a region within the duct where the local fluid velocity is opposite to the mean fluid flow.

References

Barletta, A., 2001. Analysis of flow reversal for laminar mixed convection in a vertical rectangular duct with one or more isothermal walls. Int. J. Heat Mass Transfer 44, 3481–3497.

Barletta, A., 2002. Fully developed mixed convection and flow reversal in a vertical rectangular duct with uniform wall heat flux. Int. J. Heat Mass Transfer 45, 641–654.

Barletta, A., Zanchini, E., 1999. On the choice of the reference temperature for fully-developed mixed convection in a vertical channel. Int. J. Heat Mass Transfer 42, 3169–3181.

Cheng, C.-H., Weng, C.-J., Aung, W., 1995. Buoyancy effect on the flow reversal of three-dimensional developing flow in a vertical rectangular duct—a parabolic model solution. ASME J. Heat Transfer 117, 236–241.

Cheng, C.-H., Weng, C.-J., Aung, W., 2000. Buoyancy-assisted flow reversal and convective heat transfer in entrance region of a vertical rectangular duct. Int. J. Heat Fluid Flow 21, 403–411.

Gao, S.X, Hartnett, J.P., 1993. Analytical Nusselt number predictions for slug flow in rectangular duct. Int. Commun. Heat Mass Transfer 20, 751–760.

Gau, C., Yih, K.A., Aung, W., 1992. Reversed flow structure and heat transfer measurements for buoyancy-assisted convection in a heated vertical duct. ASME J. Heat Transfer 114, 928–935.

Hartnett, J.P., Kostic, M., 1989. Heat transfer to Newtonian and non-Newtonian fluids in rectangular ducts. Adv. Heat Transfer 19, 247–356.

Hwang, G.J., Tzeng, S.C., Soong, C.Y., 2001. A computer-aided parametric analysis of mixed convection in ducts. Int. J. Heat Mass Transfer 44, 1857–1867.

Lee, K.-T., 1999. Laminar natural convection heat and mass transfer in vertical rectangular ducts. Int. J. Heat Mass Transfer 42, 4523–4534.

McBain, G.D., 1999. Fully developed laminar buoyant flow in vertical cavities and ducts of bounded section. J. Fluid Mech. 401, 365–377.

Shah, R.K., London, A.L., 1978. Laminar forced convection in ducts. In: Irvine, T.F., Hartnett, J.P. (Eds.), Advances in Heat Transfer. Academic Press, New York.

Spiga, M., Morini, G.L., 1996. Nusselt numbers in laminar flow for H2 boundary conditions. Int. J. Heat Mass Transfer 39, 1165–1174.